Available online at www.sciencedirect.com

ScienceDirect

Procedia Manufacturing 26 (2018) 1230–1241

Procedia MANUFACTURING

www.elsevier.com/locate/procedia

46th SME North American Manufacturing Research Conference, NAMRC 46, Texas, USA

Multi-Sensor Data Analytics for Grinding Wheel Redress Life Estimation- An Approach towards Industry 4.0

Kalpana Kannan, N. Arunachalam*, Aakash Chawla, Sundararajan Natarajan

Department of Mechancial Engineering, Indian Institute of Technology, Chennai 600 036, India

* Corresponding author. Tel.: +91-442-257-4722; fax: +91-442-257-4652.
E-mail address: chalam@iitm.ac.in

Abstract

Grinding is an expensive and complex machining process, characterized by cutting grits undergoing non-uniform wear. The worn out grits influence the surface finish of the part, necessitating timely dressing. Conventionally, the dressing interval is decided either based on the wheel life end criteria viz. visual identification of the workpiece burn mark, chatter occurrence and deterioration in the part finish or on the number of parts produced. Improper dressing interval increases auxiliary machining time and grinding wheel wastage. Prevailing demands towards next generation smart manufacturing include product and process related benefits such as low operational cost, better customer service support, operation optimization and control. In the present work, we propose a low cost, process non-intrusive sensor technology with IoT enabled operational intelligence platform to estimate the redress life of grinding wheel based on wheel condition. Traverse grinding tests were carried out in a CNC surface grinding machine installed with Al_2O_3 wheel against D2 tool steel under wet condition. During experimentation, the spindle motor current, grinding forces and grinding wheel surface images were acquired using the Hall-effect sensor, dynamometer, and CCD camera respectively. Data acquisition, network connectivity, and cloud communication were empowered by serial output. Statistical time, frequency and wavelet domain features signifying the wheel life characteristic were extracted. To show the usefulness of motor current signals, the extracted features thereof were confirmed against grinding forces and wheel surface images. A time series Auto-Regressive Moving Average (ARMA) predictive model was developed to estimate the grinding wheel redress life using the selected root mean square (RMS) feature of a current signal. An android application was also developed for a graphical visualization of dressing time based on the RMS value of the spindle motor current signal. The developed methodology thus, allows operators and machines with sensors to communicate with each other and facilitates real-time traceability, visibility and control over the dressing action to perform automatic dressing before the wheel reaches its end of life.

Peer-review under responsibility of the scientific committee of the 46th SME North American Manufacturing Research Conference.

Keywords: Traverse grinding; Wheel wear; Spindle motor current, Redress life, IoT manufacturing.

2351-9789
Peer-review under responsibility of the scientific committee of the 46th SME North American Manufacturing Research Conference.
10.1016/j.promfg.2018.07.160

1. Introduction

Manufacturing industries demand increased productivity with high precision and accuracy. Grinding is one such technique widely used to meet the aforementioned criteria. A typical grinding wheel is composed of randomly distributed abrasive grits embedded in a binding matrix. The material process is based on abrasive machining process. The quality of the process is dependent on wheel topography and deviation in the wheel profile leads to a loss in the desired workpiece quality. Thus, the wheel dressing of grinding wheel is essential after specific tool life. Dressing causes wheel loading which primes to faster wheel wear. Commonly in the shop floor, the dressing interval is decided by the operator based either on the end of wheel life criteria such as burn marks, chatter occurrence, deterioration of part finish or on the number of parts produced. Both of these are not precise. This is because, in the former, the part surface damage and the dimensionality error occur whereas, in the latter, the grinding wheels are not utilized to its maximum life; thus frequent dressing causes the grinding wheel wastage and increases in the process time and the overall cost. It is thus necessary to propose a structured dressing of the grinding wheel based on the instantaneous wheel condition. This can be achieved through wheel condition monitoring [1-2].

Several researchers have carried out condition monitoring of grinding wheel using several static and dynamic monitoring methods. Chai and Rowe [3] reviewed three different topography measurement methods using vitrified CBN grinding wheels. The interferometer and the laser triangulation method were best suited for three dimensional measurements of the small and the large area of both the wheel and the replica respectively. Darafon et al., [4] introduced a three dimensional non-contact wheel scanning system to measure and characterize the grinding wheel topography. It was observed that the cutting edge width and the spacing were exponentially distributed whilst the protrusion height was normally distributed.

Arunachalam and Ramamoorthy [5] performed texture analysis of grinding wheel wear assessment using machine vision technique. The texture analysis methods based on the histogram, grey level co-occurrence method (GLCM) and grey level average parameter (Ga) were used on the images to quantify the significant change in the texture of the grinding wheel. Arunachalam and Vijayaraghavan [6] used texture features of the grinding wheel images to determine the number of passes required to dress the grinding wheel. It was observed from the images, the bright spots in the images or the percentage loaded areas decreased with increasing number of dressing passes.

Lezanski [7] proposed an intelligent system for condition monitoring of the grinding wheel using AE sensor, vibration meter, and piezoelectric transducer. ANN and neuro-fuzzy models were developed to classify the condition of the grinding wheel. It was concluded that for the development of a fuzzy logic system with many input variables, the neuro-fuzzy algorithm is the only effective application. The performance of such system could be lower than the neural network system due to its limited potential to extract the knowledge from the fuzzy rule base. Moreover, in such systems, the performance index decreases increasing set of rules. Eun-Sang et al., [8] used the spindle motor current and AE signals to investigate the plunge grinding process and established its relationship with the grinding material removal rate in terms of the infeed rate. The variations in the motor current with the grinding parameters were also discussed. It was observed that the measured motor current is directly proportional to the infeed rate and the wokpiece velocity, whilst it is inversely proportional to the grinding speed. For practical applications, spindle motor current information is preferable over AE energy signal.

Yao et al., [9] have used complex continuous wavelet coherence technique which combines the cross wavelet transform (XWT) and the wavelet coherence (WTC) to perform a quantitative correlation analysis of the motor current and the chatter vibration in grinding. It was established that as the chatter occurs during grinding, a clear inner correlation between the motor current and the chatter vibration is observed. Karpuschewski.et.al. [10] developed a condition monitoring system based on power and AE sensors. The FFT of the enveloped AE signal was analyzed by using a three-layered back propagation neural network. This has been used to detect the disturbances and for wheel life estimation. A fuzzy based system that combines the AE and the power signals were

deployed for optimizing the grinding cycle. Kwak and Ha [11] detected the dressing time for the grinding using tool dynamometer based on the discrete wavelet decomposition. It was observed that the grinding force increased linearly up to a 45th piece of the specimen. Further, machining decreased the grinding force due to wheel dulling and wheel loading. Thus the critical limit of the wheel was measured.

A revolution of next-generation smart manufacturing, "Internet of Things" (IoT) has emerged in a profound manner. IoT based manufacturing include process and product-related benefits such as lower operational costs, better customer or service support, operation optimization and control, product or service improvement and innovation, better supply chain management and logistics. From a service perspective, customer satisfaction and time to repair metrics are the main focuses of manufacturers. The shop floor workers, have an increasing amount of data, however, they struggle to quickly interpret the data representation. Thus, there is a lack of connects between the shop floor and the execute suite in providing real-time analytics to the key decision makers [12-13]. It is thus essential to include IoT enabled operational intelligence platform with connected products to bridge the gap between the real-time machine-level data to the business intelligence to deal with increasing market complexity, demand variability, and machine accuracy.

Starly et al., [14] have built a virtual machine tool (digital twin) by fusing manufacturing process and the sensor data information as a step towards cyber-physical manufacturing. The developed digital twin was tested on a milling machine. The system aims at diagnosis, prognosis, and optimization by virtual machine tool integration, to enhance the accuracy and the operating capability of the machine. However, as the data storage is limited to local PC, the developed system lacks accessibility to multiple remote users. Pellegrino et al., [15] have reported the important findings in the Prognostics and Health Management (PHM) manufacturing techniques, metrics, performance assessment, infrastructure and expansion to smart manufacturing. It is mentioned that the high-level goal for PHM infrastructure must include diagnosis and prognosis maintenance with 95% uncertainty, unrestricted data access and management, adaptive security and easily configurable and portable software tools. The priority challenges with the present infrastructure lie with the development of a budgetary system which includes retrofittable sensors, open source model, and timely information access. Ray [16] has discussed the state of art of present IoT architectures based on various domains namely physical, network, application, cloud service, etc. Based on cloud services, several IoT architectures such as IoTMaaS (Monitoring as a Service), IoTPaaS (Platform as a Service), IoTIaaS (Infrastructure as a Service), and IoTSaaS (Software as a Service have been reviewed. IoTPaaS is seen to be popular among others due to its domain independency support, runtime deployment of application tool and API's, multiple tenancy management and integration with other web services and databases.

Many researchers have made efforts in the - (a) measurement of wheel topography, (b) analysis of the effect of wheel wear on the grinding performance, (c) modeling of grinding wheel wear, (d) detection of dressing time and (e) the development of intelligent manufacturing system. However, no commercially successful system is available for in-process redressing of the grinding wheel with the IoT communication platform. The proposed work differs from the existing literature in the following aspects: (1) Grinding wheel wear analysis during traverse surface grinding is studied; (2) Online monitoring and detection of grinding wheel redress life using process non-intrusive low-cost sensor technology is developed; (3) Data analytics of motor current signal in various domains such as time, frequency, time-frequency and entropy measures are performed; (4) A predictive model for the grinding wheel redress life estimation is proposed and (5) IoT platform with cloud service and Android application to track, visual and control dressing action based on wheel condition is developed as an approach towards present industrial evolution.

2. Material and Methods

2.1. Experimental set-up

Grinding experiments were carried out in a CNC Chevalier surface grinding machine under wet grinding condition. The specimens made of D2 tool steel with initial dimensions 50 x 35 x 20 (mm) were ground using Al_2O_3 grinding wheel during the experiments. Stock removal of 1mm divided in to roughing (20μm), semi-finishing (10μm) and finishing

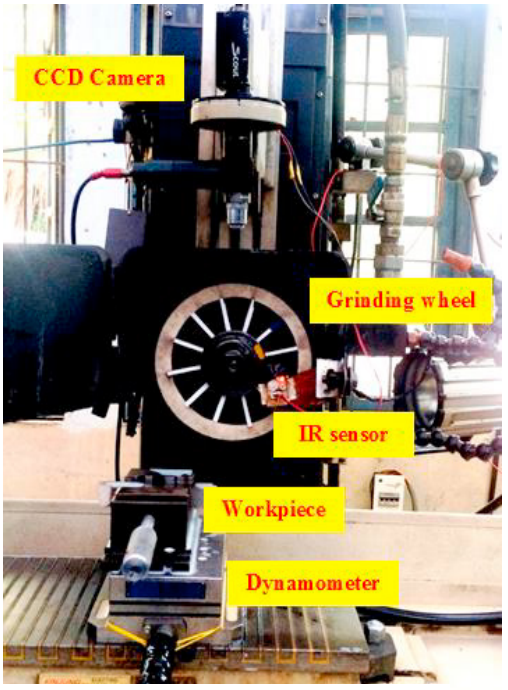

Fig. 1. Experimental set-up

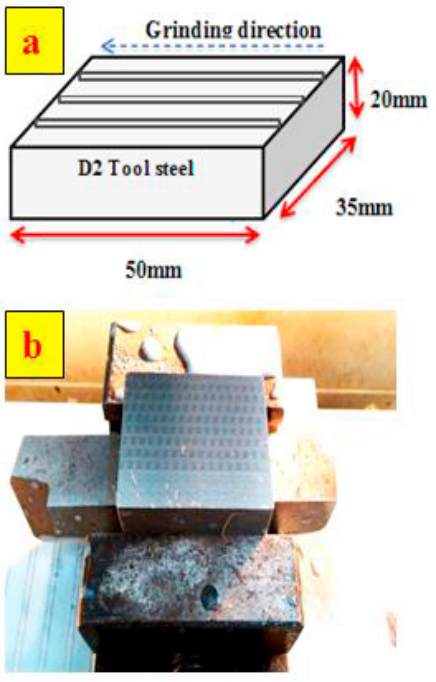

Fig. 2. (a) Grinding direction; (b) Workpiece burn mark occurrence

Table 1. Experimental Conditions

Parameters	Operating Conditions
Type of Grinding	Traverse
Tool	
Wheel specification	AA46K5V8
Wheel Outer Diameter	180 mm
Wheel Bore Diameter	31.75 mm
Workpiece	
Material	D2 Tool steel
Length	50 mm
Width	35 mm
Thickness	20 mm
Grinding parameters	
Wheel velocity	2500 rpm
Workpiece velocity	8 m/min
Depth of cut	Roughing (20µm, 2 passes)
	Semi-Finishing (10µm, 4 passes)
	Finishing (5µm, 4 passes)
Dressing tool	Diamond tip single point
Dressing feed rate	0.2 mm/rev
Dressing depth	0.01 mm
Grinding environment	Wet
Coolant	Water soluble oil (20:1)

(5µm) operations on each specimen. Before the start of experiment, the grinding wheel was dressed using a single point diamond tip dresser. A schematic representation of the experimental setup is shown in Fig. 1. and the corresponding grinding conditions [17] are listed in Table 1. The 9257B Kistler dynamometer was fixed to the grinding table over which the workpiece was mounted. LEM 25-PA current transducers were wound around each wires of the 3 phase asynchronous spindle motor. The wheel surface images were acquired using a CCD digital camera. To ensure the same positioning of the image acquisition, an infra-red based position sensor was attached to the wheel guard.

2.2. Signals and Image Acquisition

During the grinding operation, material removal was carried out along one direction as shown in Fig. 2a. For each workpiece, spindle motor current and grinding forces were measured for 30s with 16 KHz sampling frequency. The measured signals were transferred to a PC for further processing.

Consecutively, the grinding wheel surface images after each grounded workpiece were captured at 12 different positions in the wheel periphery. The acquired images were then transferred through frame grabber and stored in PC for further processing. The experiments were continued until a burn mark which signifies the end of wheel life is observed on the workpiece as shown in Fig. 2b.

3. Multi-domain signal analyses

3.1.1 Current Signal Denoising

The spindle motor current analyses were performed considering 1st, 3rd and 6th passes of grinding. However, the results are shown only for the 6th pass. Based on the minimum entropy and the maximum energy criteria [18-19], in the present study, level 5 of Daubechies wavelet is selected to perform the signal denoising. Fig. 3 shows the original and the de-noised spindle motor current signals of the 6th pass. The de-noised signal has been analyzed further in the time domain to study the variation in motor current signal for changing grinding characteristics over the number of workpieces.

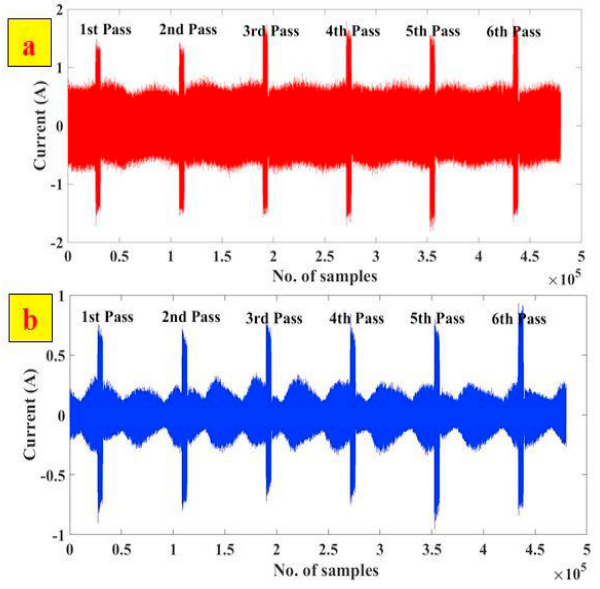

Fig. 3. (a) Original; (b) De-noised current signal

3.2.2. Time Domain Analysis

The time domain indices such as RMS, variance, kurtosis, skewness, shape factor and crest factor of motor current signals were evaluated. It is observed, that the changing trend of RMS is more evident. This is because, as the spindle motor current during roughing draws higher current due to increased material removal, thus increased force. Also during semi-finishing and finishing, less material removal results in less force and hence drop in the motor current of the grinding spindle is observed. Fig. 4. shows the grinding wheel spindle motor current variation for varying depth of cuts (20µm, 10µm, and 5µm). The motor current signal at varying depth of cuts showed fluctuating trend till 7th workpiece. These fluctuations are due to one of the following: (a) wear flat, (b) loading, (c) self-sharpening effects of the cutting edges. The useful life limit of the grinding wheel is confirmed by a substantial increase in the motor current RMS signal after the 7th workpiece at which burn marks on the ground workpieces are witnessed.

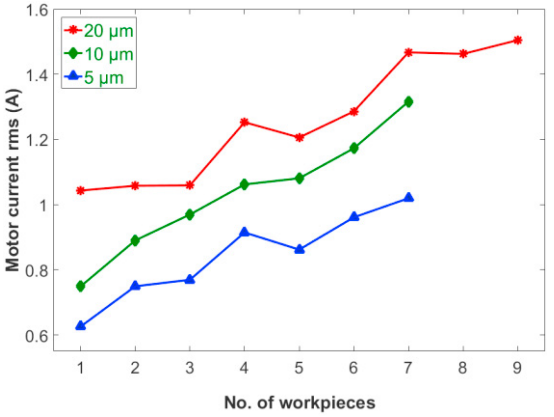

Fig. 4. Variation in grinding spindle motor current for different depths of cut over number of workpieces

In the time domain analysis, RMS is proven to be varying with the grinding wheel performance and found to track the dressing time more evidently than the other time domain features. Though the time domain parameter (RMS) is popularly used in real time due to its simplicity and lesser time complexity [20], to obtain more information on the measured current signal and to confirm that the increase in the RMS is solely dependent on wheel degradation, rather than the drop in the supply voltage or the motor overload or failures in the rotor and the stator windings [21], frequency and time-frequency domains analyses have been carried out.

3.2.3. Frequency Domain Analysis

Any undesirable events such as drop in the supply voltage, bearing failure, winding failures shows a

significant peak at respective frequencies along with the supply frequency and the harmonic content of the current signal in the frequency domain. The power spectral density (PSD) of the spindle motor current is computed as shown in Fig 5. Dominant peaks are observed only at supply (50Hz) and harmonics frequencies (100Hz, 150Hz). Thus, from the PSD it is evident that the increase in the RMS is purely due to the wheel degradation.

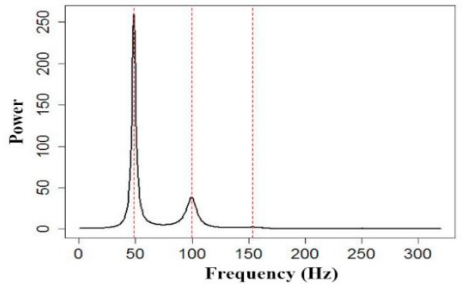

Fig. 5. Power spectral density of grinding spindle motor current signal

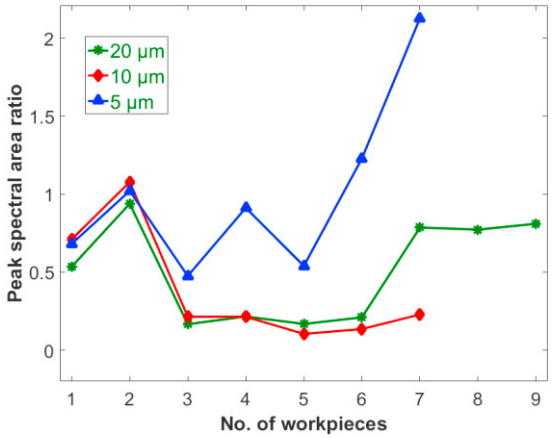

Fig. 6. Variation in first peak spectral area ratio of grinding motor current for varying depth of cut over number of workpieces

Further, it was observed that the changing trend of peak spectral area ratio is more obvious, with varying wheel characteristics against the number of workpieces. Fig. 6. shows the variation in the spectral area ratio of PSD of the motor current signal for different depth of cuts (20µm, 10µm, and 5µm) over the grinding life period. At the initial stage of grinding zone, the grinding force is unstable; hence an increase in the spectral ratio was observed at workpiece 2. Further, as the workpiece conforms to the wheel, a steady state was reached, where the forces remain almost constant and thus the spectral ratio maintains minimum variation. Whereas, it is evident that after the 7th workpiece, where burn marks were witnessed on the workpieces, a sharp sustained increase in spectral area ratio was observed due to increased force indicating the end of wheel life.

3.2.4. Wavelet Analysis

Wavelet transform supports multi-resolution analysis and represents short time interval with precise high-frequency details and lengthy time interval with low-frequency details [22]. The measured motor current signal is decomposed into 7 levels approximate (A7) and detailed (D7) coefficients using db5 wavelet. The detailed coefficients of each level were compared and it was found that the approximate and detailed coefficients of 6th and 7th levels had a clear signal over time with reduced noise. Hence, the wavelet decomposed components of the 6th and 7th levels were combined in the reconstruction of the signal. Features such as energy, variance were computed from the reconstructed signal. It was observed that, the energy variation over the number of workpieces showed a clear trend compared to that of other features. Fig. 7. shows the wavelet energy variation for different depth of cuts over the number of workpieces. In the present observation, the wavelet energy revealed that the critical wear instant begins at the 7th workpiece, where a burn mark occurrence on the workpiece is seen.

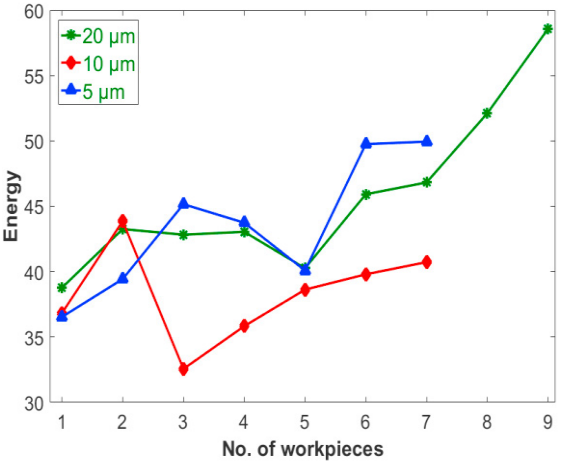

Fig. 7. Variation in wavelet energy of motor current for varying depth of cuts over number of workpieces

3.2.5. Entropy Measures

Different entropies such as approximate entropy, Shannon entropy, sample entropy, fuzzy entropy, permutation entropy, conditional entropy and corrected conditional entropy were computed for the motor current signals. It was observed that the Shannon Entropy showed more significant variation

with wheel characteristics over the grinding period than the other measured entropies. Fig. 8. shows the variation in the motor current Shannon entropy over increasing workpieces for different grinding stages (roughing, semi-finishing and finishing). With grinding time, the grinding wheel undergoes attrition wear and loading which results in the motor current signal irregularity. A rapid drop of Shannon Entropy from the 5th to the 6th workpiece followed by a sustained decrease after the 7th workpiece (burn mark occurred) during roughing clearly depicts the end of wheel life.

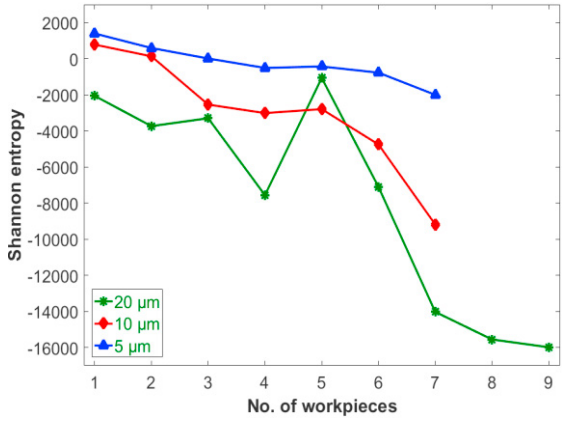

Fig. 8. Variation in Shannon entropy of motor current for varying depth of cuts over number of workpieces

From the above analyses four features namely, RMS, peak spectral area ratio, energy and Shannon entropy were observed to signify the wheel characteristics effectively over the grinding period. To select the best feature among the extracted features prognostic metrics such as monotonicity, prognosability and trendability were evaluated.

3.2.6. Prognostic metrics evaluation

The best feature among the extracted features such as the spindle motor current RMS, peak spectral area ratio, energy and Shannon entropy is selected based on the following ideal prognostic parameters such as monotonicity (m), prognosability (p) and trendability (t) [23-24]. The prognostic parameters evaluated for the extracted features for different depth of cuts are tabulated in Table 2. The results clearly depict that, at all grinding stages (roughing, semi-finishing, finishing), the motor current RMS value is observed to have high monotonicity, prognosability and trendability characteristics than that of peak spectral area ratio, energy, and Shannon entropy. It was also verified that the motor current RMS variation is purely based on wheel degradation by performing frequency and time-frequency domain analysis. This attributes that the motor current RMS feature has the advantage of perfectly representing the grinding wheel end of life information over varying operating conditions without any need of prior knowledge.

Table 2. Prognostic Metrics

Depth of cut (µm)	Motor current features	m	p	t
20	RMS	0.5	0.872	0.961
	Peak spectral area ratio	0.25	0.326	0.260
	Energy	0.859	0.693	0.5
	Shannon Entropy	0.625	0.752	0.863
10	RMS	1	0.928	0.985
	Peak spectral area ratio	0.33	0.685	0.722
	Energy	0.203	0.387	0.833
	Shannon Entropy	0.571	0.786	0.930
5	RMS	0.833	0.904	0.958
	Peak spectral area ratio	0.33	0.62	0.657
	Energy	0.833	0.725	0.67
	Shannon Entropy	0.833	0.892	0.952

4. Wheel Surface Image Analysis

The wheel surface images acquired during the grinding tests are shown in Fig. 9. Wide optical characteristic discrimination between the abrasive, the bond and the metal chip in the grinding wheel is observed due to the variation in the intensity of the reflected light. The image size of 768 x768 with grey scale range 0-255 is used in the analysis.

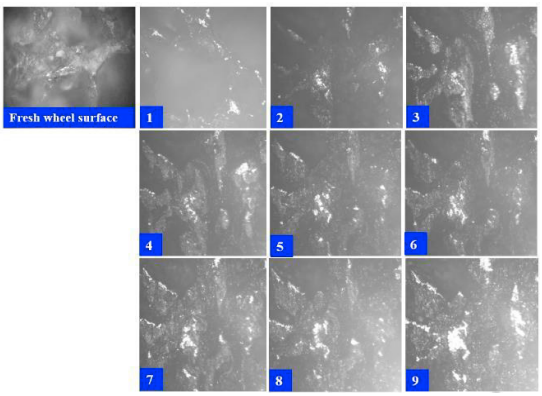

Fig. 9. Grinding wheel surface images

4.1. Image Processing

Image processing is carried out to identify the intrinsic features signifying the end of wheel life. Fig. 10. shows the illustration of each steps carried out in processing the grinding wheel surface images. The original wheel surface image as shown in Fig. 10a is segmented by region growing technique. Fig. 10b shows the segmented image which clearly defines the abrasive wear flats or loaded metal chips from background due to its high pixel intensities.

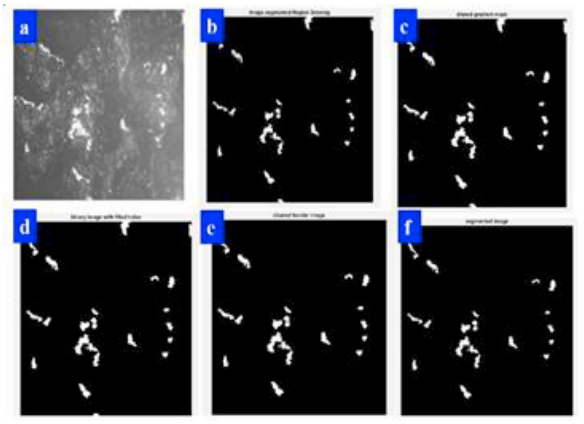

Fig. 10. (a) Original image; (b) Region-Growing Segmented image; (c) Loaded image; (d) Dilated image; (e) binary hole filled image; (f) smoothened image

Image threshold is applied to discriminate between wheel loadings and wear flat percentage in the wheel surface based on variation in their pixel intensities. As the metal chip adhered to the wheel has high pixel intensity than the wear flat, the grey scale pixel intensity greater than 250 is considered as loaded particle. The wear flat pixel intensity range is considered between 150 and 250. Fig. 10c shows the loaded image discriminated from wear flat by threshold. The image is further dilated as shown in Fig. 10d to evidently define the loaded region. Fig. 10 shows the binary image with filled holes forming closed contour pixel outlining well defined chip loaded area. Finally, the image is smoothened as shown in the Fig. 10f.

4.2. Percentage variation in loaded and wear flat areas to wheel surface

a) Wheel loading

Fig. 11. shows the processed images that illustrate the loaded area variation over the grinding period. The percentage of loaded area is computed from the processed image by dividing the pixels of area of interest by total number of pixels of the image. The percentage variation of loaded area over the period of end of wheel life is plotted in Fig. 13. As the number of pores in a newly dressed wheel is more, a gradual increase in loaded percentage at the initial stages of grinding is observed. The sudden drop in the loaded percentage at the 5th workpiece indicates the dislodgment of loaded debris due to its stack up effect. Rapid increase in wheel loading percentage is observed after the 7th workpiece, where burn mark is observed on the workpiece.

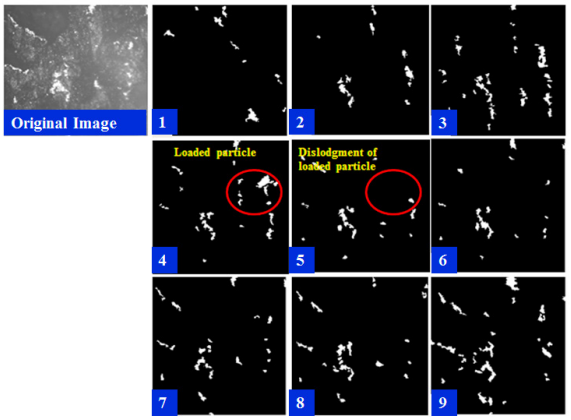

Fig. 11. Grinding wheel surface loaded images over number of workpieces

b) Wear flat

Wear flats in grinding are due to rubbing action of abrasive cutting edges against the workpiece. Over the period of grinding, the cutting edges losses its cutting ability results in glaze flat areas. These glaze flats have

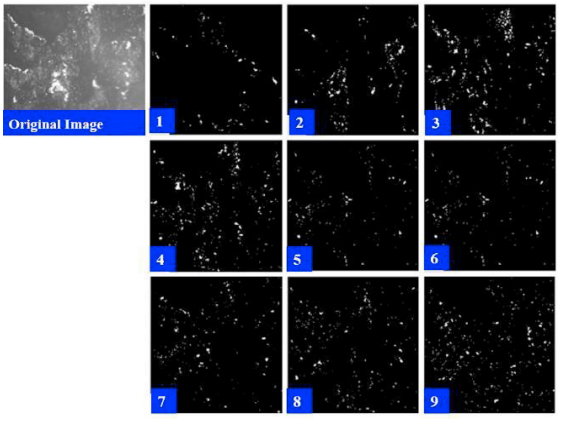

Fig. 12. Percentage loaded wheel load and wear flat to the grinding wheel over number of workpieces

pixels with high grey scale values as the polished surface of the wear flats reflects more light. The percentage of wear flat area is calculated by dividing the number of white pixels present in the wear flat area by total number of pixels of the image. Fig. 12 shows the processed images showing wear flat areas. The percentage variation of wear flat area over the period of end of wheel life is plotted in Fig. 13. The wear flat percentage is observed to increase gradually till 7th workpiece. After the 7th workpiece, burn mark occurrence is observed on the workpiece where the percent wear flat areas increased rapidly.

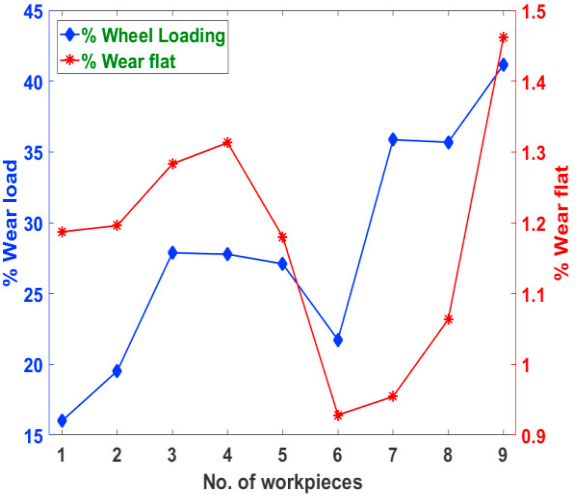

Fig. 13. Percentage loaded wheel load and wear flat to the grinding wheel over a number of workpieces

5. Redress life Model development and Validation

5.1 Auto-Regressive Moving Average

ARMA model combines Auto-Regression and Moving Average methods to predict a well behaved time series data. ARMA considers time series as stationary and assumes its approximate uniform fluctuate approximately uniform around the time-invariant mean. Thus, ARMA is more adequate for prediction of stationary time series. In the present work, though grinding is a stochastic process, the motor current RMS utilized in the development of redress life model exhibits stationarity in time series as the signals were recorded at a discrete equally spaced time interval. Thus in the present work, an ARMA model, used for modeling and forecasting univariate linear time series data, is developed to anticipate the grinding wheel redress life estimation. An AR(a) model of order 'a' uses a linear combination of the past 'a' observations of the time series along with a random error component to model the future values. MA(m) model, uses the past 'm' error components to model the future values. ARMA (a, m) forecasting model for time series v(t) is given by [25-26],

$$v(t) = H(q^{-1})e(t) \quad (1)$$

$$H(q^{-1}) = \frac{1+\sum_{i=1}^{a} c_i q^{-1}}{1+\sum_{i=1}^{a} d_i q^{-1}} \quad (2)$$

where, $H(q^{-1})$ is a lag or shift operator, e(t) is the unpredictable ideal random component at time t, 'a' and 'm' represents orders of AR and MA model, c_i, and d_i represents the coefficients of AR and MA model respectively.

Based on the minimum Normalized Mean Square Error criterion [27], ARMA (3, 3) model is chosen to predict the grinding wheel redress life before the wheel reaches its end of life. The forecast length is considered as 5. Fig. 14. shows the time series predicted motor current RMS values for different depth of cuts (20µm, 10µm, 5µm) signifying the redress time of the grinding wheel. Table 3 shows the measured and predicted values of last 5 data points of the motor current RMS. The threshold is fixed based on burn mark occurrence observed on the workpiece during grinding.

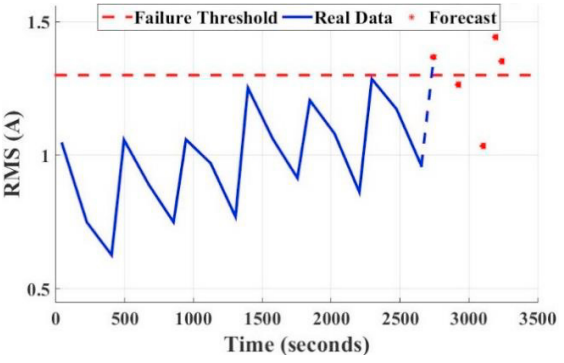

Fig. 14. Prediction of grinding wheel redress life

Table 3. Experimental runs and results

Time (s)	Predicted (RMS)	Actual (RMS)
2745	1.375	1.467
2925	1.224	1.316
3105	0.928	1.012
3195	1.370	1.462
3240	1.413	1.501

5.2. Validation

To ascertain the validity of the developed model, further 2 sets of experiment were performed for the same operating conditions as tabulated in Table 1. Fig. 15. shows the measured RMS values for 20µm depth of cut of the three experimental runs. In the second and third runs, burn marks were observed at 6th and 8th workpieces respectively. The Fit Percent of the predicted value to the measured value evaluated by Normalized Root Mean Square and the gained residual error expressing the differences between the measured and estimated behavior given by Mean Square Error (MSE) were chosen to validate the developed model [27]. The evaluated Fit Percent and MSE for the three experimental runs are tabulated in Table 4.

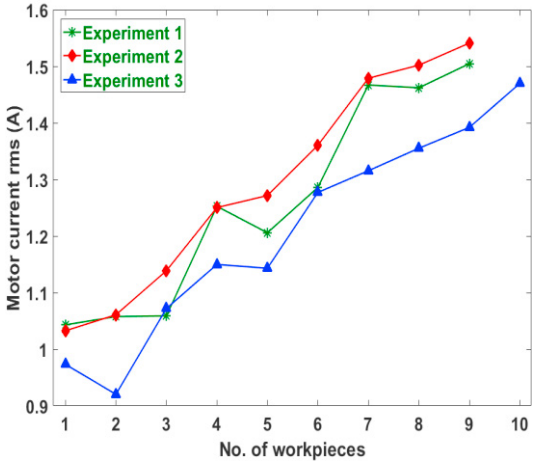

Fig. 15. Comparison of motor current RMS for 3 sets of experiments

$$FPT = 100 * \left(\frac{1-|Predicted-Actual|}{Predicted}\right)\% \quad (3)$$

$$MSE = (Predicted - Actual)^2 \quad (4)$$

Table 4. Experimental runs and results

Experiments	FPT (%)	MSE
1	75.87	0.0084
2	72.58	0.0103
3	75.48	0.0075

6. Development of IoT platform

Based on cloud services, IoT architectures are categorized as IoTMaaS, IoTPaaS, IoTIaaS, and IoTSaaS. IoTPaaS are found to be widespread among other architectures due to the following salient features [16],

- Allows connectivity of any physical devices to the IoT platform, supports any IoT transmission protocol over various communication network and thus provides domain independent services.
- Enables rapid development and deployment of runtime, application tools and API's based on client application requirement.
- Allows concurrent users to provide control over device capability, cloud resources and application management through virtualization due to its multiple tenancy ability.

In the present work, IoTPM2.5 architecture, based on IoTPaaS, is chosen for the development of IoT platform [28]. Fig. 16. shows the architecture of the developed IoT platform. It consists of five layers, namely the physical layer, the transport layer, the processing layer, the application layer and the business layer. The physical layer integrates the sensors where the information of the grinding wheel is recorded. In the transport layer, the sensed information along with the machining details are transferred to a local PC where the information is processed. The processed information is later communicated through a wireless gateway module to the IoT cloud server. The IoT cloud server is a type of Internet-based computing service that provides shared computer storage and information access to other devices or computers on demand. Any further processing of the information can also be carried out in the gateway. The information thus stored in the IoT cloud can be accessed anytime from anyplace and can trigger the control of dressing system to enable automatic dressing based on the wheel condition.

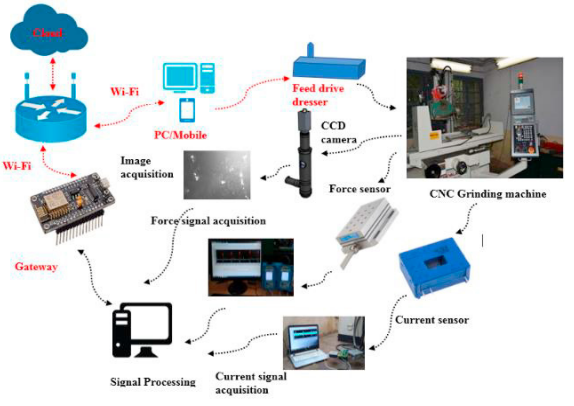

Fig. 16. IoT architecture

7. Results and Discussion

7.1. Reliability evaluation of prognostic parameter

The usefulness and the reliability of the identified prognostic parameter of the spindle motor current are validated by wheel surface images and grinding forces. Fig. 17. shows the comparative results of motor current RMS, the percentage grinding wheel surface wear flat area and the grinding forces variation over the number of workpieces for different depth of cuts.

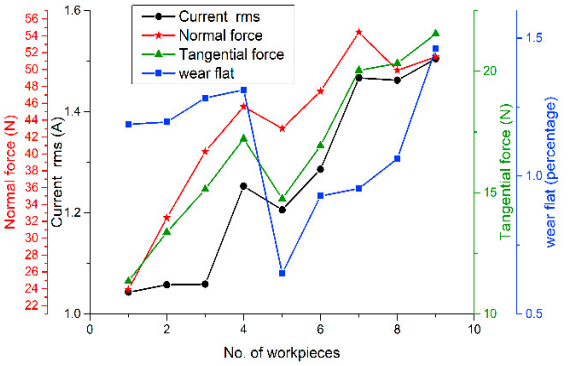

Fig. 17. Motor current RMS, Grinding forces, Percentage Wear flat, variation over number of ground workpieces

It is apparent from the above graphs that the motor current RMS follows trends similar to grinding force and the percentage wear flat area. It is also observed that the motor current RMS effectively differentiates the roughing, semi-finishing and finishing stages of grinding. Thus the motor current RMS is proven to be an effective prognostic parameter in the estimation of grinding wheel redress life.

7.2. Prediction Accuracy

From Table 4, it is observed that the fit percentage between the predicted and measured motor current RMS shows about 75% accuracy with a minimum mean squared error. Thus predicted values of motor current RMS are observed to have a good correlation with the measured motor current RMS. Hence the developed model will be useful in predicting the dressing life of the grinding wheel before the wheel reaches the end of the life.

7.3. Real-Time tracking and graphical visualization of dressing time

For real-time tracking and visualization of grinding wheel redress time, IoT cloud server based android application is developed using Android Studio 2.3.2. The information on prognostic parameter variation over the number of workpieces processed in the local host is

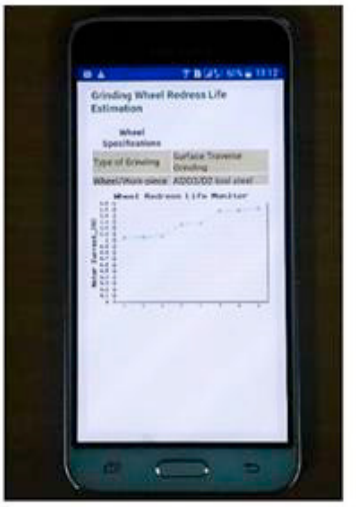

Fig. 18. Grinding wheel redress life estimation- Android application

transferred and stored to the cloud server. The developed android application shown in Fig.18. allows real-time tracking and graphical visualization of prognostic parameter variation during grinding and allows decision makers to make an instant decision on grinding wheel redress time.

8. Conclusion

In this study, a remote system to detect the grinding wheel redress life using a cost-effective sensor technology has been developed. Based on the results, the following conclusions are drawn,

- Low cost, simple installation, and process non-intrusive monitoring efficiency of the current sensor allows development of economical and effective grinding wheel condition monitoring system.
- Based on prognostic metrics (Monotonicity, Prognosability, and Trendability) evaluation, RMS of the spindle motor current was found to be an effective grinding wheel redress life prognostic parameter.
- Multi-domain signal analyses evidence that RMS variation is solely due to wheel degradation.
- The usefulness of motor current RMS variation in assessing the grinding wheel end life during various grinding stages (Roughing,

Semi-Finishing, and Finishing) was confirmed by comparing with grinding wheel surface images and grinding forces.

- The time series ARMA model was developed and validated to predict the grinding wheel redress life with 75% prediction accuracy with motor current RMS as an input.
- An IoT platform was developed which allows integration of sensor information, processes information and operators to communicate with each other and facilitate real-time traceability and visibility on grinding wheel redress life from anyplace and control over the dressing unit to perform automatic dressing before the wheel reaches its end of life. Thus, prevents and maintains the part quality with specific surface tolerance.

References

[1] K. Wegener, H.W. Hoffmeister, B. Karpuschewski, et al., Conditioning and monitoring of grinding wheels. CIRP Annals - Manufacturing Technology, 60(2), (2011) 757–777.

[2] F. Klocke, J. Thiermann, P. Mattfeld, Influence of the dressing process on grinding wheel wear. Production Engineering, 9(5–6), (2015) 563–568.

[3] R. Cai, W.B. Rowe, Assessment of vitrified CBN wheels for precision grinding. International Journal of Machine Tools and Manufacture, 44(12–13), (2004) 1391–1402.

[4] A. Darafon, A. Warkentin, R. Bauer, Characterization of grinding wheel topography using a white chromatic sensor. International Journal of Machine Tools and Manufacture, 70 (2013) 22–31.

[5] N. Arunachalam, B. Ramamoorthy, Texture analysis for grinding wheel wear assessment using machine vision. Proceedings of the Institution of Mechanical Engineers, Part B: Journal of Engineering Manufacture, 221(3), (2007) 419–430.

[6] N. Arunachalam, L. Vijayaraghavan, Assessment of grinding wheel conditioning process using machine vision. IEEE Conference on Prognostics and Health Management (PHM), (2014) 1–5.

[7] P. Lezanski, Intelligent system for grinding wheel condition monitoring. Journal of Materials Processing Technology, 109 (3), (2001) 258-263

[8] E.S. Lee, J. D. Kim, N. H. Kim, Plunge grinding characteristics using the current signal of spindle motor. Journal of Materials Processing Technology, 132, (2003) 58-66.

[9] Y. Liu, X. Wang, J. Lin, W. Zhao, Correlation analysis of motor current and chatter vibration in grinding using complex continuous wavelet coherence. Measurement Science and Technology, 27, (2016) 1-13.

[10] B. Karpuschewski, M. Wehmeier, I. Inasaki, Grinding monitoring system based on power and acoustic emission sensors. Annals of CIRP, 49(1), (2000) 235-240.

[11] J.S. Kwak, M.K. Ha, Detection of dressing time using the grinding force signal based on the discrete waveletdecomposition. International Journal of Advanced Manufacturing Technology, 23(1–2), (2004) 87–92.

[12] Y. Zhang, G. Zhang, J. Wang, S. Sun, S. Si, T. Yang, Real time information capturing and integration framework of the internet of manufacturing things. International Journal of Computer Integrated Manufacturing, 28, (2014) 811-822.

[13] Y. Lu, J. Cecil, An Internet of Things (IoT)-based collaborative framework for advanced manufacturing. The International Journal of Advanced Manufacturing Technology, 84 (5-8), (2016) 1141-1152.

[14] Y. Cai, B. Starly, P. Cohen and Y.S. Lee, Sensor data and information fusion to construct digital-twins virtual machine tools for cyber-physical manufacturing, Procedia Manufacturing, (2017) 1031-102.

[15] J.Pellegrino, M. Jusstiniano, A. Raghunathan, Measurement science roadmap for prognostics and health manssagement for smart manufacturing systems. NIST Advanced Manufacturing, (2016).

[16] P.P. Ray, A survey on Internet of Things archietectures, Journal of King Saud University-Computer and Information Sciences, (2016).

[17] B.B. Fathallah, N.B. Fredj, H. Sidhom, C. Braham, Y. Ichida, Effects of abrasive type cooling mode and peripheral grinding wheel speed on the AISI D2 steel ground surface integrity. International Journal of Machine Tools and Manufacture, 49, (2009) 261-272.

[18] Z. A. Jaffery, K. Ahmad, P. Sharma, Selection of Optimal Decomposition Level Based on Entropy for Speech Denoising using wavelet packet. Journal of Bioinformatics and Intelligent control, 1, (2013) 196-202.

[19] M. Alfoouri, K. Daqrouq, ECG signal denoising by Wavelet transform thresholding. American Journal of Applied Science, 5(3), (2008) 276–281.

[20] N. Subrahmanya, Y.C. Shin, Automated Sensor Selection and Fusion for Monitoring and Diagnostics of Plunge Grinding. Journal of Manufacturing Science and Engineering, 130(3), (2008) 310-314.

[21] M.Seera, C.P. Lim, Dhaman Ishak, H. Singh, Fault detection and diagnosis of induction motor using motor current signature analysis and a hybrid FMM-CART model. IEEE transcation on Neural networks and learning system, 23(1), (2012) 97-108.

[22] Z. Yang, Z. Yu, Grinding wheel wear monitoring based on wavelet analysis and support vector machine. International Journal of Advanced Manufacturing Technology, 62(1–4), (2012) 107–121.

[23] J. Coble, J.W. Hines, Identifying optimal prognostic parameters from data: a genetic algorithms approach. Proceedings of the Annual Conference of the Prognostics and Health Management Society, (2009) 1–11.

[24] F. Barbieri, J.W.Hines, M. Sharp, M. Venturini, Sensor based degradation prediction and prognostics for remaining useful life estimation: validation on experimental data of electric motors. International Journal of Prognostics and Heath Management, (2015).

[25] D.Djurdjanovic,, J.Yan, H.Qiu, J.Lee, J.Ni, Web-enabled remote spindle monitoring and prognostics.(2003).

[26] C.M. Stralkowski, S.M. Wu, R. E. Devor, Characterization of grinding wheel profiles by autoregressive moving average models, International Journal of Machine Tool Design and Research, 9(2), (1969) 145-163.

[27] D.C. Swanson, Signal processing for intelligent sensor systems with MATLAB, 2nd Edition

[28] P.P. Ray, Internet of Things Cloud Based Smart Monitoring of Air Borne PM2.5 Density level, SCOPES, (2016) 32-35. P.P. Ray, Internet of Things Cloud Based Smart Monitoring of Air Borne PM2.5 Density level, SCOPES, (2016) 32-35.